Non-resonant electrostatic energy harvester for wideband applications

Ling Bu[1,2], *Xiaoming Wu*[1,2], *Xiaohong Wang*[1,2], *Litian Liu*[1,2]

[1]*Institute of Microelectronics, Tsinghua University, Beijing, People's Republic of China*
[2]*Tsinghua National Laboratory for Information Science and Technology, Beijing, People's Republic of China*
E-mail: buling08@mails.tsinghua.edu.cn

Published in Micro & Nano Letters; Received on 3rd December 2012; Revised on 28th January 2013; Accepted on 1st February 2013

Presented is a novel non-resonant electrostatic energy harvester targeted at the wideband frequency response for micro-system powering. To boost non-resonance power output under low frequency, the vertical gap changing method is adopted to induce variable charges, which generates approximately 17 times of charge change compared with the conventional method of laterally changing overlap area (at 1 mm gap). Further, to boost the low frequency and non-resonant power generating capability, the differential structure is adopted to achieve doubled output voltages. Testing results reveal that optimal output power occurs when the inner plate is of large effective movement range and large relative displacement with surrounding electrets. Maximally, 3.9–7.0 V voltage and 0.2–0.7 μW power are achieved over the 5–120 Hz frequency range.

1. Introduction: The burgeoning applications such as wireless sensor networks and implantable medical equipment [1], have presented grave powering challenges. Plenty of terminals are to be powered, and most of these terminals are not only remotely distributed but also hard to access. Conventional powering methods such as wiring and batteries can hardly meet the requirements because of infrastructure limits and finite lifespan, etc.

Vibration energy harvesting, on the other hand, presents an alternative solution to the above powering issue. As at present, various vibration energy harvesters have been reported, including piezoelectric, electromagnetic and electrostatic [2–4]. Most of these reported energy harvesters are based on resonant structures such as cantilevers [5] or spring-mass-damper systems [6], with resonant frequencies typically around the order of ~1 kHz [5–7]. However, in a real environment, vibrations are usually of varying and low frequencies (typically below 100 Hz) [8, 9]. Specifically, the frequency of human-induced motions can be as low as 1–10 Hz [9]. Thus, the power generation performances of resonant energy harvesters are limited when utilised in low frequency and wideband applications, regardless of transduction mechanisms.

In this Letter, we present a novel non-resonant electrostatic energy harvester for low frequency and wideband applications. Unlike previous literature [2–11], we eliminate the resonant structures such as springs and introduce a freestanding movable electrode, and thus the energy harvester is inherently non-resonant. The vertical gap changing method and differential structure are adopted to boost power out at low frequency and at non-resonance. The details are explained in following Sections.

2. Device design: The design of the proposed device is shown in Fig. 1. The non-resonant energy harvester consists of three metal plates which form two capacitors, C_{up} and C_{bottom}. The inner plate is freestanding, and is movable due to external vibrations [12]. Both the upper and bottom electrodes are attached with electrets. When the inner plate moves upward, the amount of induced charges on the upper electrode decreases, and correspondingly the generated current flows through resistance R_1 into ground. At the same time, the amount of induced charges on the bottom plate increases, which results in current flowing from ground through resistance R_2, and vice versa. In vibration, vertical gaps of C_{up} and C_{bottom} vary alternatively, and the corresponding change of induced charges produces a differential AC current on external load resistors.

Compared with the conventional lateral capacitive structure, the proposed non-resonant energy harvester adopts the vertical gap changing method to generate current. The principle of the vertical gap changing method is based on electrostatic equilibrium. For the parallel capacitor, the electric field between capacitor electrodes is determined at a specific gap value, and accordingly the amount of induced charges on the electrodes is determined. Therefore, the gap between capacitor electrodes are of critical importance in generating induced charges and voltage on external load resistances. Equation (1) shows the relation between generated voltage and capacitor gap value:

$$V = R \cdot \frac{\mathrm{d}Q}{\mathrm{d}t} = R \cdot \frac{\mathrm{d}Q}{\mathrm{d}g} \cdot \frac{\mathrm{d}g}{\mathrm{d}t} \tag{1}$$

where Q is the amount of induced charges, R is load resistance and g is the gap between two electrodes. For sinusoidal vibration, $(\mathrm{d}g/\mathrm{d}t)_{max} = A_{vib}\omega_{vib}$, where A_{vib} and ω_{vib} are the amplitude and angular frequency of external vibration, respectively. Assuming that maximal voltage V_{MAX} occurs when $(\mathrm{d}g/\mathrm{d}t)$ reaches maximal, then V_{MAX} is proportional to the derivative of induced charges with respect to the gap value, that is $(\mathrm{d}Q/\mathrm{d}g)$.

Fig. 2 exhibits the normalised output voltage with respect to the vertical gap of the capacitor (electrode area: 10×10 mm). The experimental details for Fig. 2 are as follows: one electrode with electrets is fixed, while the other electrode is vibrated by the electromagnetic shaker. The gap between the vibrating electrode and the fixed electrode is adjusted in the range of 0–5 mm by the X–Y stage, and the voltage generated by the fixed electrode at different gap values is recorded and normalised to maximum. The normalisation here is adopted to exclude testing-related parameters including load resistance R, vibration amplitude A_{vib} and angular frequency ω_{vib}. As the capacitor gap increases, voltage decreases significantly in the 1 mm range. Fitting predicts that

$$V_{MAX} \propto g^{-\alpha} \tag{2}$$

where V_{MAX} stands for normalised maximal voltage, g for capacitor gap and $\alpha \simeq 3$.

Integrating for induced charge Q from (1), when $g \to 0$ the amount of induced charges is approximately 18 times of that when $g = 1$ mm. This indicates that, at the initial gap value of 1 mm, charge change ΔQ of the vertical method is about 17 times that of the lateral method, as is shown in the inset of Fig. 2. Thus, varying the gap vertically is a sensitive power generation method, especially in the 0–1 mm range.

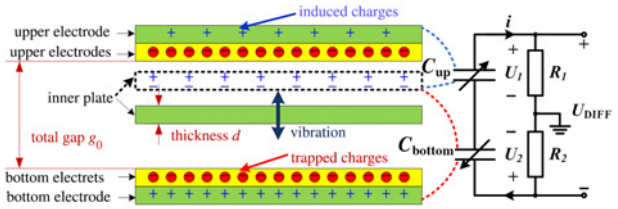

Figure 1 *Concept of non-resonant electrostatic energy harvester*

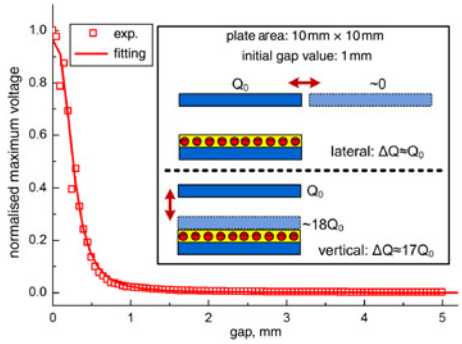

Figure 2 *Experimental normalised maximal output voltage against capacitor gap*

3. Experiments: The fabrication process of the non-resonant energy harvester is as follows: 1. thermally grow 3000 Å SiO_2 on Si wafer; 2. sputter 2000 Å Al on SiO_2 layer; 3. attach polydimethylsiloxone (PDMS) layer (cavities are predefined on the PDMS layer using moulds) to the Al layer; 4. attach polytetrapluoroethylene (PTFE) thin film (6 × 6 mm) into the PDMS cavities. After fabrication, the PTFE electrets are corona charged to approximately −400 V surface potential. In the assembly process, two identical PDMS cavities with charged PTFE electrets are adopted. A steel plate (5 × 5 mm) is inserted into one of the open cavities, and is then encapsulated using the other one. Fig. 3*a* shows the entire process flow of the fabrication, corona charging and assembly. Fig. 3*b* shows the photo of the fabricated PDMS open cavities with attached PTFE electrets on the wafer, and Fig. 3*c* shows the photo of the assembly process, with the inset showing the fabricated device and lateral dimensions.

The testing setup is shown in Fig. 4. Samples are vibrated over the 5–120 Hz frequency range using an electromagnetic shaker. The maximum acceleration imposed on the device is 2.5 g. Differential testing circuitry is adopted and the electrical signals are recorded using an Agilent 35 670 A dynamic signal analyser. The thickness of both total gap g_0 and inner plate thickness d (as is shown in Fig. 1) can be adjusted to form different samples.

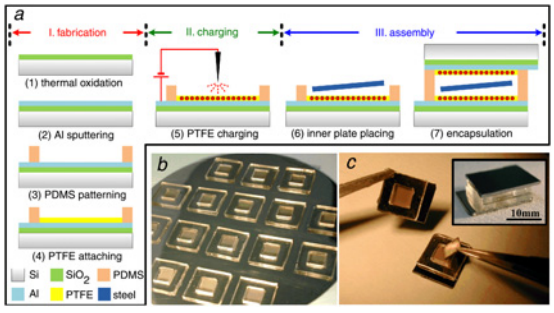

Figure 3 *Fabrication, corona charging and assembly processes of energy harvester (Fig. 3a); photo of PDMS cavities on wafer (Fig. 3b); assembly process, with inset of fabricated energy harvester (14 × 10 mm laterally) (Fig. 3c)*

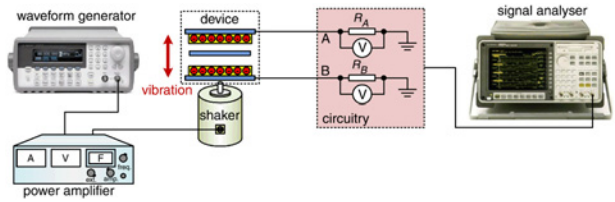

Figure 4 *Testing setup of the non-resonant energy harvester*

In this work, three sets of device parameters are adopted: 1. g_0 = 1 mm, d = 0.5 mm; 2. g_0 = 2 mm, d = 1 mm; 3. g_0 = 2 mm, d = 0.5 mm. The corresponding effective movement range of the inner plate is 0.5, 1 and 1.5 mm, respectively.

4. Results and discussion: The PTFE electrets used in this work are characterised by a scanning electron microscope (SEM) as well as the surface potential contour, as is shown in Figs. 5*a* and *b*, respectively. In the SEM image, the PTFE electrets are generally composed of sub-micron grains with tiny cracks in between. These cracks introduce additional defect energy levels and are conducive to enhance the charge trapping ability of the PTFE electrets. In Fig. 5*b*, the contour plot of the surface potential of the 6 × 6 mm PTFE electrets after corona charging (needle voltage: −6 kV, grid voltage: −400 V) is quite uniform. The average surface potential is −391 V and the standard deviation is −9.8 V.

Fig. 6 shows the voltage-time traces of both terminals and differential output at 5 and at 120 Hz. The terminal voltages are periodic and in opposite phases, while the differential voltage doubles the output voltage of a single terminal, thus proving the differential

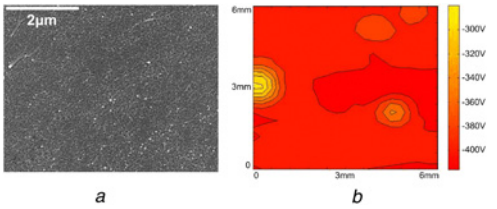

Figure 5 *SEM image of PTFE electrets, and contour plot of surface potential*
a SEM image
b Contour plot

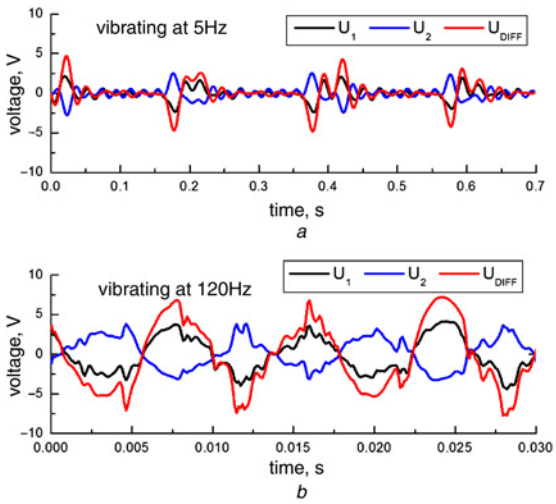

Figure 6 *Voltage-time traces of terminal and differential output*
a At 5 Hz
b At 120 Hz

doi: 10.1049/mnl.2012.0924

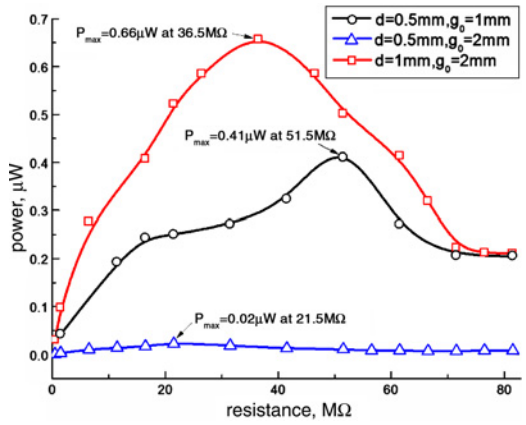

Figure 7 *Power-resistance traces of different samples*

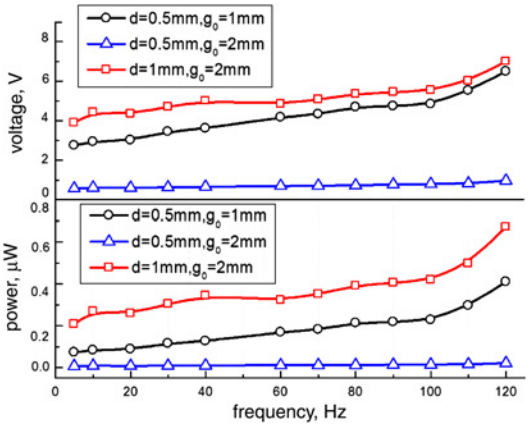

Figure 8 *Frequency responses of different samples in terms of voltage and power*

output characteristics of the energy harvester. Maximal generated voltage reaches 4.9 V at 5 Hz and 7.3 V at 120 Hz, respectively. Imperfections in periodicity of the voltage–time traces are due to the uncertain collisions between the inner plate and device casing.

Fig. 7 compares the power-resistance traces for samples with three different sets of parameters. The red curve ($g_0 = 2$ mm, $d = 1$ mm) represents the optimal device, in that the 1 mm effective movement range of the inner plate is in accordance with the most sensitive gap range shown in Fig. 2. A highest output power of 0.66 μW is achieved on a load resistance of 36.5 MΩ for this device. Compared with the red curve, the black one ($g_0 = 1$ mm, $d =$ 0.5 mm) presents less power output, mainly because the effective movement range of the inner plate is smaller than the optimal device, and this results in less induced charge amount changes. For this device, maximum power reaches 0.41 μW on a load resistance of 51.5 MΩ. The lowest power is observed for the device with parameters $g_0 = 2$ mm, $d = 0.5$ mm, and the maximal power only reaches 0.02 μW on 21.5 MΩ. Despite larger effective movement range (1.5 mm), for this device the thinner inner plate within the larger gap results in ineffective relative displacement between the inner plate and the other two electrodes. Thus, optimising the power output should be traded off between enlarging effective movement range and inducing large relative displacement for the inner plate.

Fig. 8 shows the frequency response of samples with different parameters, in terms of generated voltage and output power. As is shown in Fig. 8, for all three types of devices over the range of 5–120 Hz, output voltage and power increase as the vibration frequency increases, proving the non-resonant characteristic of all devices. For the optimal device with parameters $g_0 = 2$ and $d = 1$ mm, a highest voltage range of 3.9–7.0 V and a highest power range of 0.2–0.7 μW are generated over the 5–120 Hz, demonstrating the potential of the proposed energy harvester for wideband applications.

5. Conclusions: This Letter presents the design, fabrication and testing of a novel non-resonant electrostatic energy harvester for low frequency and wideband applications. To boost non-resonance power output under low frequencies, we adopt the vertical gap changing method to induce charges, which generates about 17 times of charge change compared with the conventional method of laterally changing overlap area (at 1 mm gap). Further, we adopt the differential structure to achieve doubled output voltage. Testing results reveal that the device with parameters $g_0 = 2$ and $d = 1$ mm presents optimal power output capability due to large effective movement range and effective relative displacement of the inner plate. Maximally, 3.9–7.0 V voltage and 0.2–0.7 μW power are achieved over the 5–120 Hz frequency range.

6. Acknowledgments: This work was supported by the State Key Development Program for Basic Research of China (Grant No. 2009CB320304), the Key Program of the Natural Science Foundation of China (Grant No. 60936003) and the Beijing Natural Science Foundation (Grant No. 3122023).

7 References

[1] Vullers R.J.M., van Schaijk R., Doms I., van Hoof C., Mertens R.: 'Micropower energy harvesting', *Solid-State Electron.*, 2009, **53**, (7), pp. 684–693

[2] Elfrink R., Renaud M., Kamel T.M., *ET AL.*: 'Vacuum-packaged piezoelectric vibration energy harvesters: damping contributions and autonomy for a wireless sensor system', *J. Micromech. Microeng.*, 2010, **20**, (10), p. 104001 (7 pages)

[3] Galchev T., Hanseup K., Najafi K.: 'Micro power generator for harvesting low-frequency and nonperiodic vibrations', *J. Microelectromech. Syst.*, 2011, **20**, (4), pp. 852–866

[4] Takahashi T., Suzuki M., Hirata T., *ET AL.*: 'Electret energy harvesting based on fringe electrical field change inside trenched ferroelectric'. Proc. MEMS'11, Cancun, Mexico, January 2011, pp. 1305–1308

[5] Boisseau S., Despesse G., Ricart T., Defay E., Sylvestre A.: 'Cantilever-based electret energy harvesters', *Smart Mater. Struct.*, 2011, **20**, p. 105013 (11 pages)

[6] Kulkarni S., Koukharenko E., Tudor J., Beeby S., O'Donnell T., Roy S.: 'Fabrication and test of integrated micro-scale vibration based electromagnetic generator'. Proc. Transducers'07 and Eurosensors XXI, Lyon, France, June 2007, pp. 879–882

[7] Ly R., Rguiti M., D'Astorg S., Hajjaji A., Courtois C., Leriche A.: 'Modeling and characterization of piezoelectric cantilever bending sensor for energy harvesting', *Sensor. Actuat. A, Phys.*, 2011, **168**, (1), pp. 95–100

[8] Najafi K., Galchev T., Aktakka E.E., Peterson R.L., McCullagh J.: 'Microsystems for energy harvesting'. Proc. Transducers'11, Beijing, China, June 2011, pp. 1845–1850

[9] Mitcheson P.D., Yeatman E.M., Rao G.K., Holmes A.S., Green T.C.: 'Energy harvesting from human and machine motion for wireless electronic devices', *Proc. IEEE*, 2008, **96**, (9), pp. 1457–1486

[10] Erturk A., Renno J.M., Inman D.J.: 'Modeling of piezoelectric energy harvesting from an L-shaped beam-mass structure with an application to UAVs', *J. Intell. Mater. Syst. Struct.*, 2009, **20**, (5), pp. 529–544

[11] Lo H.W., Tai Y.C.: 'Parylene HT for electret generators'. Proc. PowerMEMS'07, Freiburg, Germany, November 2007, pp. 57–60

[12] Veluswami M.A., Crossley F.R.E., Horvay G.: 'Multiple impacts of a ball between two plates. Part 2: Mathematical modeling', *J. Eng. Ind. – Trans. ASME*, 1975, **97**, (3), pp. 828–835